

8303735). We also acknowledge use of the Southern California Regional NMR Facility and the support of NSF Grant CHE-7916324A1.

**Registry No.** 1, 83314-27-6; 3, 95865-15-9; 4, 95865-16-0; 5, 95865-17-1; 6, 95865-18-2; 7, 95865-19-3; 8, 95865-20-6; 9, 95865-21-7; 9-*d*<sub>3</sub>, 95865-22-8; 9-<sup>13</sup>C<sub>2</sub>, 95865-23-9; 9-<sup>15</sup>N, *d*<sub>4</sub>, 95865-24-0; 10, 95865-25-1; 10-*d*<sub>3</sub>, 95892-03-8; 10-<sup>13</sup>C<sub>2</sub>, 95865-26-2; 10-<sup>15</sup>N, *d*<sub>4</sub>, 95865-27-3; 11, 95865-28-4; 12, 95865-29-5; 13, 95865-30-8; 14, 95865-31-9; 15, 95865-32-0; 16, 95892-04-9; (η-C<sub>5</sub>Me<sub>5</sub>)<sub>2</sub>Ti(CO)<sub>2</sub>, 11136-40-6; (η-C<sub>5</sub>Me<sub>5</sub>)<sub>2</sub>Ti(η-CH<sub>3</sub>C≡CCH<sub>2</sub>CH<sub>3</sub>), 95892-05-0; (η-C<sub>5</sub>Me<sub>5</sub>)<sub>2</sub>Ti(η-CH<sub>3</sub>C≡C(CH<sub>2</sub>)<sub>4</sub>CH<sub>3</sub>), 95865-33-1; (η-C<sub>5</sub>Me<sub>5</sub>)<sub>2</sub>Ti(η-CH<sub>3</sub>C≡CPh), 95865-34-2; (η-C<sub>5</sub>Me<sub>5</sub>)<sub>2</sub>TiC(CH<sub>3</sub>)=C(CH<sub>2</sub>CH<sub>3</sub>)CH<sub>2</sub>CH<sub>2</sub>, 95865-35-3; (η-C<sub>5</sub>Me<sub>5</sub>)<sub>2</sub>Ti(C(CH<sub>2</sub>CH<sub>3</sub>)=C(CH<sub>3</sub>)CH<sub>2</sub>CH<sub>2</sub>), 95865-36-4; (η-C<sub>5</sub>Me<sub>5</sub>)<sub>2</sub>TiC(CH<sub>3</sub>)=C[(CH<sub>2</sub>)<sub>4</sub>CH<sub>3</sub>]CH<sub>2</sub>CH<sub>2</sub>, 95865-37-5; (η-C<sub>5</sub>Me<sub>5</sub>)<sub>2</sub>TiC((CH<sub>2</sub>)<sub>4</sub>CH<sub>3</sub>)=C(CH<sub>3</sub>)CH<sub>2</sub>CH<sub>2</sub>, 95865-38-6; (η-C<sub>5</sub>Me<sub>5</sub>)<sub>2</sub>TiC(CH<sub>3</sub>)=C(Ph)CH<sub>2</sub>CH<sub>2</sub>, 95865-39-7; (η-C<sub>5</sub>Me<sub>5</sub>)<sub>2</sub>TiC(Ph)=C(CH<sub>3</sub>)CH<sub>2</sub>CH<sub>2</sub>, 95892-06-1; (η-C<sub>5</sub>Me<sub>5</sub>)<sub>2</sub>TiO(CH<sub>3</sub>)<sub>2</sub>CCH<sub>2</sub>CH<sub>2</sub>, 95865-40-0; [(η-C<sub>5</sub>Me<sub>5</sub>)<sub>2</sub>Ti]<sub>2</sub>(μ-N<sub>2</sub>), 11136-46-2; CO<sub>2</sub>, 124-38-9; CO, 630-08-0; Me<sub>3</sub>CC≡CH, 917-92-0; CH<sub>3</sub>CN, 75-05-8; CD<sub>3</sub>CN, 2206-26-0; <sup>13</sup>CH<sub>2</sub><sup>13</sup>CH<sub>2</sub>, 51915-19-6; propyne, 74-99-7; 2-butyne, 503-17-3; ethylene, 74-85-1; allene, 463-49-0; diphenylacetylene, 501-65-5; 2-pentyne, 627-21-4; 2-octyne, 2809-67-8; 1-phenylpropyne, 673-32-5; propionitrile, 107-12-0; 2,2-dimethylpropionitrile, 630-18-2; *p*-tolunitrile, 104-85-8; acetaldehyde, 75-07-0; acetone, 67-64-1; 2,3-dimethylcyclopent-2-enone, 1121-05-7.

**Supplementary Material Available:** Spectroscopic data for (η-C<sub>5</sub>Me<sub>5</sub>)<sub>2</sub>Ti(η-CH<sub>3</sub>C≡CR) and the corresponding isomeric metallacyclopentenes, where R = C<sub>2</sub>H<sub>5</sub>, CH<sub>2</sub>(CH<sub>2</sub>)CH<sub>3</sub>, and Ph (2 pages). Ordering information is given any current masthead page.

## Effects of the Conformational Rearrangement of the (np<sub>3</sub>)M Fragment in the Course of the Reaction between (np<sub>3</sub>)MH Hydrides [M = Co, Rh; np<sub>3</sub> = N(CH<sub>2</sub>CH<sub>2</sub>PPh<sub>2</sub>)<sub>3</sub>] and Carbon Disulfide

Claudio Bianchini,\* Dante Masi, Carlo Mealli,\* Andrea Meli, and Michal Sabat

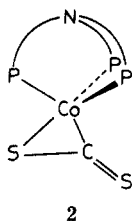
*Istituto per lo Studio della Stereochimica ed Energetica dei Composti di Coordinazione, C.N.R., 50132 Firenze, Italy*

Received June 25, 1984

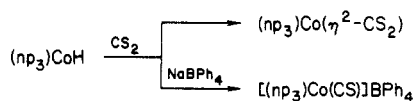
The reactivity of the complex (np<sub>3</sub>)RhH toward CS<sub>2</sub> has been investigated. Depending on the presence or absence of NaBPh<sub>4</sub> in the reaction mixture, two different compounds are obtained: [(np<sub>3</sub>)Rh(η<sup>2</sup>-CS<sub>2</sub>)]BPh<sub>4</sub>·0.5C<sub>2</sub>H<sub>5</sub>OH and (np<sub>3</sub>)Rh(S<sub>2</sub>CH). In contrast to the rhodium hydride, the cobalt analogue is reported to yield [(np<sub>3</sub>)Co(CS)]BPh<sub>4</sub> and (np<sub>3</sub>)Co(η<sup>2</sup>-CS<sub>2</sub>). An indirect way of obtaining a stable rhodium analogue of the cobalt thiocarbonyl complex is presented. The structure of the Rh(I)-η<sup>2</sup>-CS<sub>2</sub> complex has been determined by X-ray diffraction analysis in order to compare its stereochemical features with those of the Co(0) analogue: *a* = 19.134 (3) Å, *b* = 17.061 (3) Å, *c* = 9.111 (1) Å, α = 83.95 (2)°, β = 79.70 (1)°, γ = 84.46 (1)°, triclinic, *P*1̄, *Z* = 2. In the complex cation the (np<sub>3</sub>)M fragment distorts from the common C<sub>3v</sub> symmetry by accommodating two phosphorus atoms in trans axial positions of an octahedron; the nitrogen and the third phosphorus atoms lie cis to each other in the equatorial plane. This arrangement corresponds to the shape of typical L<sub>4</sub>M fragments with C<sub>2v</sub> symmetry where d<sup>8</sup> metal fragments of this type are supportive of η<sup>2</sup>-CS<sub>2</sub> coordination. Although the four different products obtainable from the reaction of the cobalt and rhodium hydrides with CS<sub>2</sub> indicate multiple-reaction pathways, there is enough evidence that these may be caused by the ease of the rearrangement of the (np<sub>3</sub>)M fragment and by the amphoteric nature of the (np<sub>3</sub>)MH hydrides. This paper, by referring to a series of experimental and theoretical observations for complexes containing the (np<sub>3</sub>)M fragment, offers suggestions as to how one can interpret major, different trends of the reactivity. Qualitative MO arguments, supported in some cases by EHMO calculations, are used to check whether the existence of the proposed key intermediates is allowed or not.

### Introduction

In a recent paper we described CS<sub>2</sub> chemistry of a reactive metal hydride, namely, the complex (np<sub>3</sub>)CoH, 1 [np<sub>3</sub> = tris(2-(diphenylphosphino)ethyl)amine].<sup>1</sup> Depending on the presence of NaBPh<sub>4</sub> in the reaction mixture, two different products can be obtained: (i) a para-



### Scheme I



magnetic cobalt(0) complex, (np<sub>3</sub>)Co(η<sup>2</sup>-CS<sub>2</sub>), which was assigned the structure 2; (ii) a cobalt(I) thiocarbonyl complex, [(np<sub>3</sub>)Co(CS)]BPh<sub>4</sub>, 3, as shown in Scheme I.

The unique bonding capabilities of the ligand np<sub>3</sub> must play an important role in determining the different reactivities of (np<sub>3</sub>)CoH. In effect, the ligand envelopes the metal in different modes that ultimately affect the mobility of hydrogen over the coordination sphere and hence the different modes of rupture of the M-H linkage.<sup>2,3</sup> This

(1) Bianchini, C.; Meli, A.; Scapacci, G. *Organometallics* 1983, 2, 1834.

(2) Bianchini, C.; Masi, D.; Mealli, C.; Meli, A.; Sabat, M.; Scapacci, G. *J. Organomet. Chem.* 1984, 273, 91.

determines the amphoteric nature of the hydrogen ligand.

In order to learn more about the reactivity of this type of system, we have investigated the behavior toward  $CS_2$  of the rhodium analogue of 1, i.e.,  $(np_3)RhH$ , 4.<sup>4</sup> Two major products have been isolated and characterized:  $(np_3)Rh(S_2CH)$ , 5, and  $[(np_3)Rh(\eta^2-CS_2)]BPh_4 \cdot 0.5C_2H_5OH$ , 6, respectively. A chemical-physical characterization of the latter products, which includes an X-ray study of 6, shows that the chemistry of this rhodium hydride is markedly different from that of the cobalt analogue.

In this paper we report the experimental results and outline some general ideas about the origin of the multi-form reactivity of  $(np_3)MH$ . No kinetic studies of the reactions could be performed. A detailed mechanistic study is complicated by the numerous variables required to define possible reaction pathways and by the fact that most intermediates lack any symmetry. Nonetheless, the previously developed arguments for the electronic features of typical  $CS_2$  complexes<sup>5</sup> and a qualitative fragment orbital analysis<sup>6</sup> of important intermediates (in some cases supported by EHMO calculations<sup>7</sup>) are used to establish possible keypoints in the chemistry of these reactive metal hydrides. The reader is informed that the following considerations are not intended to establish a mechanistic theory for very complicated reactions; rather they provide insight, based upon well-developed bonding theory, for the observed patterns of the various reactions.

## Results

**Synthesis of the Compounds.** Though complete structural data for 4 are not available, this complex has been assigned the same structure as the trigonal-bipyramidal cobalt(I) derivative 1.<sup>8</sup> The two compounds share a number of chemical properties including the reactivity toward  $CO_2$ <sup>9</sup> but react differently with  $CS_2$ . At variance with 1 which forms complex 2, 4 reacts with  $CS_2$  yielding the dithioformate rhodium(I) complex 5. This is obtained as red diamagnetic crystals by adding  $CS_2$  to a THF suspension of 4 (yield 50%). It is reasonably air stable in the solid state but decomposes rapidly in common organic solvents unless air is excluded. In this case it behaves as a nonelectrolyte. The IR spectrum contains no  $\nu(Rh-H)$ , but there are absorptions at 1220 and 960  $cm^{-1}$ , which we assign to  $\nu(HCS)$  and  $\nu(CS_2)_{asym}$  of a dithioformate ligand.<sup>10,11</sup> A positive assignment for  $\nu(CS_2)_{asym}$  is not possible because the region 800–700  $cm^{-1}$  is partially masked by vibrations associated with the phosphine ligand. The <sup>1</sup>H NMR spectrum in  $CD_2Cl_2$  is also consistent with the presence of the dithioformate ligand showing a resonance at 9.60 ppm.<sup>10</sup> The <sup>31</sup>P{<sup>1</sup>H} NMR spectrum ( $CD_2Cl_2$ , -60 °C) exhibits a doublet at 23.6 ppm ( $J_{P-Rh} = 156$  Hz). This

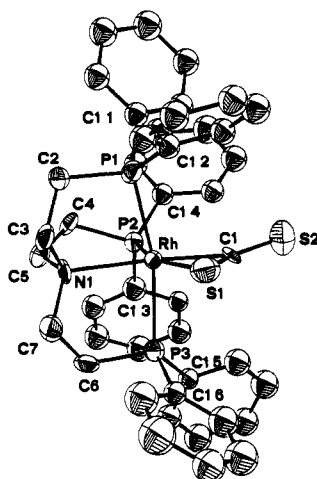
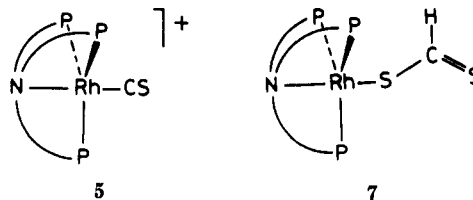


Figure 1. ORTEP drawing of the  $[(np_3)Rh(\eta^2-CS_2)]^+$  complex cation.

pattern is consistent with rapid intramolecular exchange of the three phosphorus atoms, as commonly found in  $np_3$  complexes where the tripodal ligand behaves as tetradentate.<sup>1</sup> On the basis of all of these data it is reasonable to assign the structure shown below to 5.



Orange crystals of  $[(np_3)Rh(\eta^2-CS_2)]BPh_4 \cdot 0.5C_2H_5OH$ , 6, are obtained in 18% yield when  $NaBPh_4$  is added to the mother liquor of the reaction leading to 5. Compound 6 is diamagnetic and air stable both in the solid state and in solution. It is soluble in common organic solvents, in which it behaves as a 1:1 electrolyte (molar conductance value in  $10^{-3}$  M nitroethane solution 45  $\Omega$   $cm^2$   $mol^{-1}$ ). The IR spectrum shows two bands at 1155 and 640  $cm^{-1}$  which, by comparison with a variety of  $\eta^2-CS_2$  metal complexes, have been assigned to the out-of-ring  $\nu(C=S)$  and to the in-ring  $\nu(C-S)$  stretching vibrations, respectively.<sup>1,12</sup> No band in the region 2800–2850  $cm^{-1}$  is present, thus indicating that the nitrogen atom is coordinated to the metal center.<sup>1</sup> The <sup>31</sup>P{<sup>1</sup>H} NMR spectrum ( $CD_2Cl_2$ , 20 °C) exhibits a typical  $AB_2X$  pattern, very similar to that shown by the complex  $[(np_3)RhCl_2]BPh_4$  which was assigned an octahedral geometry.<sup>4</sup> The X-ray structural analysis, presented below, confirms the quasi-octahedral geometry of 6. Finally, it is worth mentioning, also for comparative purposes, that although no thiocarbonyl species are formed in the reaction of 4 with  $CS_2$ , a stable complex of formula  $[(np_3)Rh(CS)]BPh_4$ , 7, is obtained as orange crystals by treatment of a  $[RhCl(C_2H_4)_2]_2/np_3$  mixture with  $TiPF_6$  followed by addition of  $CS_2$ . The compound is air stable both in the solid state and in solution. It is soluble in common organic solvents, in which it behaves as a 1:1 electrolyte (molar conductance value in  $10^{-3}$  M nitroethane solutions 46  $\Omega$   $cm^0$   $mol^{-1}$ ). The IR spectrum shows a strong band at 1300  $cm^{-1}$  assigned to the  $\nu(CS)$  stretching vibration of a terminal thiocarbonyl group.<sup>1</sup> The <sup>31</sup>P{<sup>1</sup>H}

(3) Cecconi, F.; Ghilardi, C. A.; Innocenti, P.; Mealli, C.; Midollini, S.; Orlandini, A. *Inorg. Chem.* 1984, 23, 922.

(4) Di Vaira, M.; Peruzzini, M.; Zanobini, F.; Stoppioni, P. *Inorg. Chim. Acta* 1983, 69, 37.

(5) Mealli, C.; Hoffmann, R.; Stockis, A. *Inorg. Chem.* 1984, 23, 56.

(6) Albright, T. A. *Tetrahedron* 1982, 38, 1339 and references therein.

(7) Hoffmann, R. *J. Chem. Phys.* 1963, 39, 1397. Hoffmann, R.; Lipscomb, W. H. *Ibid.* 1962, 36, 3179, 3489; 1962, 37, 2872. Information about local utilities for calculations is given in ref 3, which also contains some details on modeling of the  $np_3$  ligand in the various geometries. The parameters used for cobalt and rhodium are those reported in: Albright, T. A.; Hoffmann, P.; Hoffmann, R. *J. Am. Chem. Soc.* 1980, 99, 7546 (for Co). Pinhas, A. R.; Albright, T. A.; Hoffmann, P.; Hoffmann, R. *Helv. Chim. Acta* 1980, 63, 29 (for Rh).

(8) Sacconi, L.; Ghilardi, C. A.; Mealli, C.; Zanobini, F. *Inorg. Chem.* 1975, 14, 1380.

(9) Bianchini, C.; Meli, A. *J. Am. Chem. Soc.* 1984, 106, 2698.

(10) Bianchini, C.; Innocenti, P.; Meli, A.; Orlandini, A.; Scapacci, G. *J. Organomet. Chem.* 1982, 233, 233 and references therein.

(11) Gattow, G.; Behrendt, W. *Top. Sulfur Chem.* 1977, 2.

(12) (a) Yanoff, P. V. *Coord. Chem. Rev.* 1977, 232, 183. (b) Bianchini, C.; Mealli, C.; Meli, A.; Orlandini, A.; Sacconi, L. *Inorg. Chem.* 1980, 19, 2968. (c) Bianchini, C.; Masi, D.; Mealli, C.; Meli, A. *Inorg. Chem.* 1984, 23, 2838.

Table I. Summary of Crystal Structure Data

formula	$C_{67}H_{62}BS_2P_3NRh \cdot 0.5C_2H_5OH$
$M_r$	1175.05
cryst form	red parallelepiped
cryst size, mm	$0.325 \times 0.105 \times 0.05$
cryst system	triclinic
space group	$P\bar{1}$
$a$ , Å	19.134 (3)
$b$ , Å	17.061 (3)
$c$ , Å	9.111 (1)
$\alpha$ , deg	83.95 (2)
$\beta$ , deg	79.70 (1)
$\gamma$ , deg	84.46 (1)
$V$ , Å <sup>3</sup>	2900.8 (3)
$Z$	2
$d(\text{calcd})$ , g cm <sup>-3</sup>	1.345
$\mu(\text{Mo K}\alpha)$ , cm <sup>-1</sup>	4.81
radiant	graphite-monochromated Mo K $\alpha$ , $\lambda = 0.71069$ Å
scan type	$\omega/2\theta$
$2\theta$ range, deg	5–46
scan width, deg	0.8
scan speed, deg s <sup>-1</sup>	0.06
total data ( $\pm h, \pm k, l$ )	7940
unique data $I > 3\sigma(I)$	3009
no. of parameters	262
$R$	0.076
$R_w$	0.076
$\omega = 1.0[\sigma^2(F_o) + pF_o^2]^{-1}$	$p = 0.0012$

NMR spectrum (CDCl<sub>3</sub>, 20 °C) exhibits a doublet at 39.44 ppm ( $J_{P-Rh} = 144$  Hz). These data are in good agreement with those found for the trigonal-bipyramidal cobalt

analogue **3**, which has been studied through X-ray methods.<sup>2</sup> It is therefore reasonable to assign to **7** a trigonal-bipyramidal geometry.

**Description of the X-ray Structure.** The structure consists of discrete cations  $[(np_3)Rh(\eta^2-CS_2)]^+$  and tetraphenylborate anions. Figure 1 shows an ORTEP drawing of the complex cation. Selected bond lengths and angles are summarized in Tables III and IV. As expected from the chemical-physical characterization of the complex, the metal is coordinated by all four donor atoms of the ligand  $np_3$  and by one C–S linkage of  $CS_2$ . The geometrical features of the Rh– $CS_2$  fragment compare well with those found in other transition-metal complexes containing  $CS_2$ <sup>12</sup> if the differences between the metal radii are taken into account. Nonetheless the S–C–S angle of 142.2 (10)° seems slightly above average, and the distance from carbon of the noncoordinated sulfur atom [1.539 (14) Å] is slightly below average.

No X-ray structural data are available for **2**; however, this compound is comparable to the paramagnetic cobalt(0) complex (triphos)Co( $\eta^2-CS_2$ ), **8** [triphos =  $CH_3C(CH_2PPh_2)_3$ ].<sup>12b</sup> In fact, since in **2** the amine group is not coordinated, the  $P_3Co^0$  fragment adopts the  $C_{3v}$  symmetry of an hemioctahedron which, for d<sup>9</sup> and d<sup>10</sup> configurations, is supportive of  $\eta^2$ -coordination for heteroallenic molecules.<sup>5</sup> Such an arrangement is found also in  $(np_3)Co(\eta^2-SCNPh)$ .<sup>12c</sup> In contrast, the  $np_3$  ligand envelopes the metal in **6** in a very different mode, destroying the  $C_{3v}$  symmetry of the  $(np_3)M$  fragment. This has only a couple of precedents, namely, the complexes  $[(np_3)Co]BPh_4$ <sup>13</sup> and

Table II. Final Positional Parameters ( $\times 10^4$ ) for  $[(np_3)Rh(CS_2)]BPh_4 \cdot 0.5C_2H_5OH$ 

atom	x	y	z	atom	x	y	z
Rh	2647 (1)	2540 (1)	6945 (2)	C15	1081 (6)	1972 (6)	9406 (15)
P1	3351 (2)	3640 (3)	6273 (5)	C25	1040 (6)	1391 (6)	10611 (15)
P2	3159 (2)	1911 (3)	4796 (5)	C35	587 (6)	1528 (6)	11954 (15)
P3	1670 (2)	1781 (3)	7617 (5)	C45	175 (6)	2245 (6)	12093 (15)
S1	2449 (3)	2897 (3)	9458 (6)	C55	215 (6)	2825 (6)	10888 (15)
S2	3671 (3)	1629 (4)	9388 (7)	C65	668 (6)	2689 (6)	9545 (15)
N1	1967 (7)	3221 (8)	5314 (16)	C16	1767 (6)	724 (7)	7712 (13)
B1	1706 (11)	6840 (12)	3540 (22)	C26	2288 (6)	347 (7)	8496 (13)
C1	3051 (7)	2182 (8)	8908 (17)	C36	2349 (6)	-476 (7)	8739 (13)
C2	2772 (9)	4329 (10)	5169 (21)	C46	1889 (6)	-921 (7)	8208 (13)
C3	2010 (9)	4083 (10)	5524 (20)	C56	1367 (6)	-544 (7)	7430 (13)
C4	2937 (9)	2676 (9)	3327 (17)	C66	1306 (6)	279 (7)	7181 (13)
C5	2214 (10)	3061 (11)	3729 (19)	C17	1198 (6)	7692 (7)	3249 (10)
C6	1143 (9)	2157 (11)	6166 (19)	C27	1071 (6)	8279 (7)	4240 (10)
C7	1194 (9)	3042 (11)	5749 (21)	C37	721 (6)	9006 (7)	3844 (10)
C11 <sup>a</sup>	4234 (6)	3634 (6)	5124 (13)	C47	499 (6)	9145 (7)	2457 (10)
C21	4407 (6)	4244 (6)	4010 (13)	C57	626 (6)	8557 (7)	1465 (10)
C31	5106 (6)	4278 (6)	3253 (13)	C67	975 (6)	7831 (7)	1861 (10)
C41	5633 (6)	3702 (6)	3611 (13)	C18	2543 (6)	6954 (6)	2610 (13)
C51	5460 (6)	3092 (6)	4725 (13)	C28	2662 (6)	7482 (6)	1330 (13)
C61	4761 (6)	3058 (6)	5483 (13)	C38	3350 (6)	7537 (6)	522 (13)
C12	3504 (5)	4137 (7)	7859 (12)	C48	3919 (6)	7063 (6)	993 (13)
C22	3157 (5)	4865 (7)	8227 (12)	C58	3800 (6)	6535 (6)	2272 (13)
C32	3304 (5)	5215 (7)	9443 (12)	C68	3112 (6)	6480 (6)	3080 (13)
C42	3798 (5)	4837 (7)	10291 (12)	C19	1371 (7)	6087 (8)	3021 (15)
C52	4146 (5)	4109 (7)	9923 (12)	C29	636 (7)	6035 (8)	3356 (15)
C62	3999 (5)	3759 (7)	8707 (12)	C39	333 (7)	5419 (8)	2871 (15)
C13	4107 (6)	1662 (7)	4322 (10)	C49	765 (7)	4854 (8)	2051 (15)
C23	4465 (6)	1247 (7)	5405 (10)	C59	1500 (7)	4907 (8)	1715 (15)
C33	5183 (6)	988 (7)	5029 (10)	C69	1803 (7)	5523 (8)	2200 (15)
C43	5543 (6)	1145 (7)	3570 (10)	C110	1754 (6)	6665 (7)	5372 (15)
C53	5185 (6)	1561 (7)	2487 (10)	C210	1331 (6)	6122 (7)	6283 (15)
C63	4467 (6)	1819 (7)	2863 (10)	C310	1349 (6)	6008 (7)	7815 (15)
C14	2841 (6)	1001 (6)	4302 (12)	C410	1790 (6)	6437 (7)	8436 (15)
C24	2439 (6)	1001 (6)	3166 (12)	C510	2213 (6)	6980 (7)	7525 (15)
C34	2264 (6)	288 (6)	2763 (12)	C610	2196 (6)	7094 (7)	5993 (15)
C44	2491 (6)	-426 (6)	3496 (12)	O1	4318 (19)	9224 (21)	1160 (39)
C54	2892 (6)	-426 (6)	4632 (12)	C8	4716 (13)	9860 (16)	605 (27)
C64	3067 (6)	288 (6)	5035 (12)				

<sup>a</sup>The carbon atoms C11 to C66 belong to the phenyl rings of the complex cation, while the atoms C17 to C610 are those from the BPh<sub>4</sub> anion.

Table III. Selected Bond Distances (Å)

Rh-S1	2.387 (5)	P2-C14	1.847 (13)
Rh-P1	2.380 (5)	P3-C6	1.829 (17)
Rh-P2	2.345 (5)	P3-C15	1.848 (14)
Rh-P3	2.332 (5)	P3-C16	1.789 (13)
Rh-N1	2.299 (12)	N1-C3	1.514 (20)
Rh-C1	2.085 (14)	N1-C5	1.483 (19)
S1-C1	1.648 (15)	N1-C7	1.513 (20)
S2-C1	1.539 (14)	C2-C3	1.526 (22)
P1-C2	1.876 (16)	C4-C5	1.475 (21)
P1-C11	1.821 (13)	C6-C7	1.525 (23)
P1-C12	1.831 (12)	B1-C17	1.692 (23)
P2-C4	1.845 (15)	B1-C18	1.691 (23)
P2-C13	1.807 (12)	B1-C19	1.637 (25)
		B1-C110	1.682 (24)

Table IV. Selected Bond Angles (deg)

S1-Rh-P1	87.5 (2)	C2-C3-N1	112.7 (14)
S1-Rh-P2	160.1 (2)	C4-C5-N1	117.7 (14)
S1-Rh-P3	88.2 (2)	C6-C7-N1	110.0 (14)
S1-Rh-N1	117.9 (4)	Rh-N1-C1	104.4 (9)
P1-Rh-P2	93.6 (2)	Rh-N1-C5	113.8 (10)
P1-Rh-P3	161.9 (1)	Rh-N1-C7	111.1 (10)
P2-Rh-P3	96.4 (2)	Rh-P1-C11	126.2 (4)
P1-Rh-N1	83.0 (4)	Rh-P1-C12	114.6 (4)
P2-Rh-N1	82.0 (4)	C11-P1-C12	110.4 (6)
P3-Rh-N1	83.5 (4)	Rh-P2-C13	122.5 (4)
S1-Rh-C1	42.6 (4)	Rh-P2-C14	123.2 (4)
P1-Rh-C1	94.6 (4)	C13-P2-C14	98.7 (5)
P2-Rh-C1	117.5 (4)	Rh-P3-C15	116.1 (4)
P3-Rh-C1	94.0 (4)	Rh-P3-C16	121.9 (4)
N1-Rh-C1	160.5 (5)	C15-P3-C16	102.6 (6)
Rh-P1-C2	101.5 (6)	C17-B1-C18	108.5 (12)
Rh-P2-C4	100.2 (6)	C17-B1-C19	111.4 (13)
Rh-P3-C6	100.9 (6)	C17-B1-C110	109.7 (12)
S1-C1-S2	143.2 (10)	C18-B1-C19	111.6 (13)
P1-C2-C3	109.5 (11)	C18-B1-C110	107.3 (12)
P2-C4-C5	111.9 (11)	C19-B1-C110	108.3 (13)
P3-C6-C7	111.9 (13)		

$[(np_3)CoCl_2]BF_4$ .<sup>14</sup> In these cases one of the P-M-P angles in **6** opens up to 161.9 (1.0)°. The two phosphorus atoms involved [P(1) and P(3) in Figure 1] are trans to each other leaving the N and P(2) atoms cis. CS<sub>2</sub> is practically coplanar with the NRhP<sub>2</sub> plane. Certainly the different electron count at the metal imposes different structures for the  $(np_3)M$  fragments in **2** and **6**, respectively. Interestingly  $np_3$  adapts with ease to the canonical fragment L<sub>4</sub>M, **9**, which, for d<sup>8</sup> species, is supportive of  $\eta^2$ -coordination of heteroallenes.



Discussion

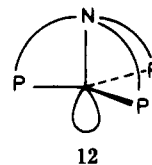
As shown in the previous sections the chemical reactivity toward CS<sub>2</sub> of  $(np_3)RhH$  differs significantly from that of the isoelectronic  $(np_3)CoH$  hydride, **1**. To summarize, in the absence of NaBPh<sub>4</sub>, **1** yields the stable paramagnetic  $\eta^2$ -CS<sub>2</sub> adduct **2**, whereas the rhodium analogue **4** yields the five-coordinate dithioformate complex **5**. By contrast the BPh<sub>4</sub><sup>-</sup> anion favors the stabilization of an  $\eta^2$ -CS<sub>2</sub> adduct of rhodium(I), **6**, but, when the metal is cobalt, forces the degradation of CS<sub>2</sub> to CS, to give compound **3** (see Scheme

I). The latter result is somewhat surprising since the thiocarbonyl of rhodium(I) **7** is a stable species itself, as shown by its easy formation, reported above.

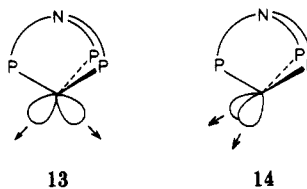
Recently we have started investigating in a general way the reactivity of compounds of the type  $(np_3)M$ , where M = d<sup>10</sup>, and  $(np_3)MX$ , where M = d<sup>8</sup> and X is a monodentate anionic ligand. There is crystallographic evidence that in these systems the  $(np_3)M$  unit may interconvert between a trigonal pyramid, **10**, and a hemioctahedron, **11**, where nitrogen is not metal coordinated.<sup>3,15,16</sup>



MO calculations show that for d<sup>10</sup> metals the interconversion is symmetry allowed and costs only a few kilocalories per mole. On the other hand, cleavage or formation of the M-N bond in  $(np_3)MX$  systems, while keeping C<sub>3v</sub> symmetry may not be reversible on account of a symmetry-imposed barrier for certain combinations of M and X. What one should be aware of is that the frontier orbitals at the metal undergo dramatic rearrangements which alter its bonding capabilities. Thus, whereas **10** has the unique  $\sigma$ -hybrid **12**, which points toward the missing apex of a



trigonal bipyramid (TBP), up to three localized hybrids pointing toward three unoccupied *fac* positions of an octahedron may be constructed for **11**. However, stable adducts of the  $(np_3)M$  fragment with more than two coligands have never been observed probably on account of the fact that, in this way, the total number of electrons may exceed the formal value 18. When two coligands (L and L') are accepted, two sets of hybrids can be envisaged as symmetry-allowed combinations of the frontier orbitals of **11**. The first localized hybrid set **13** points toward an axial and an equatorial position of the TBP while the second **14** has two  $\sigma$ -hybrids pointing toward two basal sites of a square pyramid (SP).



The TBP-SP interconversion, attainable by a 90° rotation and a slight tilting (with respect to the threefold axis) of the LML' plane, should not be expensive in terms of energy. However, since the ligands L and L' occupy two nonequivalent positions in TBP, this geometry **13** seems best suited to characterize a "regiospecificity" of the chemical reactivity. We trust this latter argument since our experiments show that from equal or similar initial species very different products are obtainable.

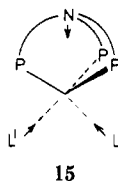
As a matter of fact, stable adducts of  $(np_3)M$  with more than one coligand generally are not stable; the apical amine

(13) Mealli, C.; Orioli, P. L.; Sacconi, L. *J. Chem. Soc. A* 1971, 2691.  
 (14) Di Vaira, M.; Meli, A.; Sacconi, L. *Cryst. Struct. Commun.* 1977, 6, 727.

(15) Ghilardi, C. A.; Mealli, C.; Midollini, S.; Orlandini, A. *Inorg. Chem.* 1985, 24, 164.

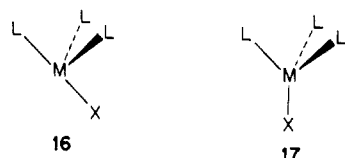
(16) Mealli, C.; Sacconi, L. *Inorg. Chem.* 1982, 21, 2870.

group of  $np_3$  is usually competing for coordination with other coligands, as schematically shown in 15.

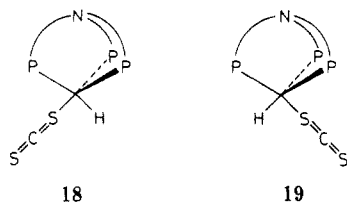


Usually the amine reenters the coordination sphere, and the  $(np_3)M$  fragment resumes shape 10, with the expulsion or migration of either L or L'. The surviving ligand shifts over the threefold axis to reform the TBP.

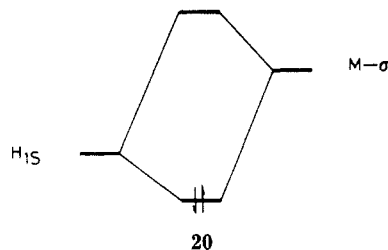
The general points discussed above should be evaluated when thinking of the reactivity of  $(np_3)MH$  species. Consider, for example, the reaction of 1 or 4 with a linear  $S=C=S$  molecule. It is reasonably assumed that as one sulfur atom of  $CS_2$  approaches the metal atom of  $(np_3)MH$ , the complex is activated in the sense that the M-N bond elongates. The problem of such an elongation in this type of molecule has been considered in detail<sup>15</sup> and is a perfectly reasonable assumption for these hydrides. Also, the hydrogen atom may bend with respect to the threefold axis of the molecule to accommodate the incoming ligand. This type of bending was shown by calculation to be a stabilizing factor for the existence of reactive diamagnetic CpML molecules ( $M = d^8$ ).<sup>17</sup> The latter species and the proposed intermediate of our hydrides, where nitrogen is not coordinated, can be assigned the same  $L_3MX$  stereochemistry shown in 16, on the basis of a well-known isolobal analogy between CpM and  $L_3M$  fragments.<sup>18</sup> Unreactive high-spin  $C_{3v}$  states, as in 17, are known both for CpML and  $(np_3)MX$  species ( $M = d^8$ ).<sup>19</sup>



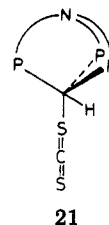
The alternative stereochemistries resulting from the addition of  $CS_2$  to 13 are shown in 18 and 19. These are the reactive intermediates that are important for the subsequent evolution of different products from the reaction between  $(np_3)MH$  and  $CS_2$ .



A very different nature (either more protonic or more hydridic) may be expected for the hydrogen atom in these two cases. Elian and Hoffmann<sup>20</sup> provided a useful suggestion: the extent of the interaction, 20, between  $H_{1s}$  and the metal  $\sigma$ -orbital is largely ruled by the energy gap argument. The higher the M  $\sigma$ -orbital, the weaker the interaction and the greater the hydrogen character of the electrons in the bonding combination; that is, the hydrogen atom is more hydridic. If applied to our problem, the argument predicts an accumulation of negative charge on the hydrogen atom, which is larger in 19 than in 18. In



fact, the metal  $\sigma$ -orbital which points toward the apex of a TBP has more  $d_{z^2}$  character than the hybrid pointing toward one of the equatorial positions. Hence it lies at lower energy. This point is confirmed by specific calculations that we have performed. Furthermore the transformation of the geometry 18 into that shown in 21 does



not require much energy while providing more protonic character to hydrogen. Note that 21 can be considered a tetrahedral complex, with an hydrogen buried in one of the faces of the tetrahedron. The metal uses one of the low-lying d lone pairs, a member of the e set, for interaction 20. Also a limiting  $d^{10}$  electron configuration is consistent with the tetrahedral geometry of the main framework of the complex. Thus the most polarized  $M^{\delta+} \cdots H^{\delta-}$  bond is expected. In other words the system 21 is the most suited to release a proton.

In summary, 19, just because the metal  $\sigma$ -hybrid pointing to hydrogen is the highest in energy, seems the best candidate for the release of hydride following the reaction of 4 with  $CS_2$ . The hydride may attack the electrophilic carbon of  $CS_2$  to yield the dithioformate complex 5. Otherwise, in presence of a bulky anion, it may definitely leave the molecule while the  $(np_3)Rh^+$  fragment rearranges to structure 9 and  $CS_2$  interconverts from end-on to side-on coordination.<sup>5</sup>

Cobalt behaves differently. In general this may be a consequence of a different basicity (or electronegativity) which corresponds to a different energy of the metal orbitals. These differences are parameter dependent and difficult to evaluate. In the formation of the  $\eta^2-CS_2$  adduct 2, hydrogen leaves as a neutral atom. This may be indicative of the minor basicity of cobalt if the reaction goes through intermediate 18. Alternatively the reaction could go through intermediate 19 or 21 which favor the accumulation of electron density at the metal. In the latter case the different reactivities of rhodium and cobalt hydrides may be considered as depending upon the regioselectivity of the  $CS_2$  attack.

After the hydrogen is eliminated, other factors become important in selecting the final routes of the reactions. Our discussion is based on recent experimental and theoretical observations reported from this laboratory.<sup>15</sup> The TBP  $(np_3)CoX$  species are stabilized as diamagnetic compounds with  $X = H$  or CN, whereas a high-spin tetrahedral structure is found for  $X =$  halide. In the latter case we have shown that the M-N distance cannot decrease beyond a certain limit on account of a symmetry-forbidden crossing between an e level and a progressively destabilized  $a_1$  level (M-N  $\sigma$ -antibonding). The latter levels are ordered as in 22 which predicts a triplet ground state for  $d^8$  species. With reference to the present problem, an intermediate

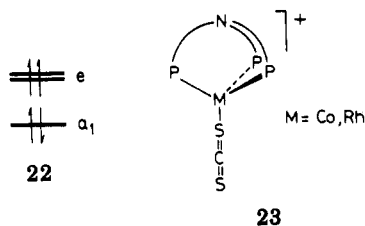
(17) Hofmann, P.; Padmanabhan, M. *Organometallics* 1983, 2, 1273.

(18) Chen, M. M.-L.; Mingos, D. M. P.; Hoffman, R. *Inorg. Chem.* 1976, 15, 1148.

(19) See ref 15 and 17 for some of the known examples.

(20) Hoffmann, R.; Elian, H. *Inorg. Chem.* 1975, 14, 1058.

of type 23 seems possible after the departure of hydridic hydrogen from 19.



For the cobalt(I) species the level order 22 persists even for short M–N distances, but a reverse ordering is calculated for the rhodium(I) analogue. Indeed there is no experimental evidence that 23 is a point along any reaction pathway; however, note that the rhodium(I) analogue would be Jahn–Teller unstable in this geometry. This may be the reason why the  $(np_3)Rh$  fragment in the structure reported in this paper, 2, does not have  $C_{3v}$  symmetry, commonly found for other  $(np_3)M$  fragments. On the other hand, cobalt is not oxidized when it forms the  $\eta^2$ -CS<sub>2</sub> adduct, and this suggests a different mechanism. Actually cobalt(I) is formed in the thiocarbonyl complex 3, but the very different nature of this product is suggestive of a reaction mechanism perhaps much more complicated.

In the light of the previous considerations we conclude that the four different products, which are formed by the reaction of CS<sub>2</sub> with very similar metal hydrides, result from fundamentally different electronic and geometric requirements encountered at certain stages along the pathways. In other words the study of the reactivity of these species cannot be treated only on the basis of different chemical nature of the metals, but a full interpretation requires a knowledge of the continuous electronic and geometric pathway.

### Experimental Section

All reactions and manipulations were carried out under a nitrogen atmosphere. Reagent grade chemicals were used in the preparations of the complexes. THF was distilled under nitrogen from sodium benzophenone ketyl. Literature methods were used for the preparation of  $(np_3)RhH^4$  and  $[RhCl(C_2H_4)_2]_2$ .<sup>21</sup> The solid complexes were collected on a sintered-glass frit and washed with appropriate solvents before being dried in a stream of nitrogen. Infrared spectra were recorded with a Perkin-Elmer 283 spectrophotometer using samples mullied in Nujol between KBr plates. <sup>1</sup>H and <sup>31</sup>P{<sup>1</sup>H} NMR spectra were taken on a Varian CFT 20 spectrometer. Peak positions are relative to tetramethylsilane and phosphoric acid, respectively, with downfield values reported as positive. Conductance measurements were made with a WTW Model LBR/B conductivity bridge.

**Reaction of  $(np_3)RhH$  with CS<sub>2</sub>.** To a suspension of  $(np_3)RhH$  (0.75 g, 1 mmol) in THF (80 mL) was added a large excess of carbon disulfide (5 mL) which caused the solid to dissolve giving a dark red solution. Within a few minutes red crystals of  $(np_3)Rh(S_2CH)$  precipitated on standing. They were filtered off and washed with THF and petroleum ether: yield 50%. Anal. Calcd for C<sub>43</sub>H<sub>43</sub>NP<sub>3</sub>RhS<sub>2</sub>: C, 61.94; H, 5.19; N, 1.68; Rh, 12.34; S, 7.69. Found: C, 61.87; H, 5.18; N, 1.71; Rh, 12.26; S, 7.58.

NaBPh<sub>4</sub> (0.34 g, 1 mmol) in butanol (30 mL) was then added to the mother liquor and the resulting solution set aside. After 3–4 days concentration at reduced pressure gave a red-orange solid which was precipitated from an acetone–ethanol mixture as orange crystals of  $[(np_3)Rh(CS_2)]BPh_4 \cdot 0.5C_2H_5OH$  in 18% yield. Anal. Calcd for C<sub>68</sub>H<sub>65</sub>BN<sub>0.5</sub>P<sub>3</sub>RhS<sub>2</sub>: C, 69.50; H, 5.57; N, 1.19; Rh, 8.76. Found: C, 69.28; H, 5.49; N, 1.20; Rh, 8.69.

**Reaction of  $[RhCl(C_2H_4)_2]_2$  with CS<sub>2</sub>.**  $[RhCl(C_2H_4)_2]_2$  (0.2 g, 0.5 mmol) and  $np_3$  (0.65 g, 1 mmol) in THF (50 mL) were

treated with TlPF<sub>6</sub> (0.39 g, 1.1 mmol) under stirring at 50 °C for 1 h. After filtration, carbon disulfide (10 mL) was added and the solution refluxed for a further 1 h. After addition of NaBPh<sub>4</sub> (0.68 g, 2 mmol) in butanol, the reaction mixture was first set aside for 3–4 days and then concentrated in vacuo. The solid material obtained was thus extracted with DMF (20 mL) and precipitated with butanol/butyl ether as orange crystals of  $[(np_3)Rh(CS)]BPh_4 \cdot DMF$  in 35% yield. Anal. Calcd for C<sub>70</sub>H<sub>69</sub>BN<sub>2</sub>OP<sub>3</sub>RhS: C, 70.47; H, 5.83; N, 2.34; Rh, 8.62; S, 2.68. Found: C, 70.29; H, 5.81; N, 2.29; Rh, 8.57; S, 2.67.

**X-ray Data Collection and Structure Determination.** A summary of crystal and intensity data is presented in Table I. All X-ray measurements were performed on a Philips PW 1100 diffractometer using Mo K $\alpha$  radiation. The cell constants and orientation matrix were determined by least-squares refinement of the setting angles for 24 reflections. The intensities of three standard reflections were measured every 120 min of X-ray exposure, and no significant decay with time was noted. The data were corrected for Lorentz and polarization effects. Numerical absorption corrections were applied with the transmission factors ranging from 0.87 to 0.91. Atomic scattering factors were those tabulated by Cromer and Waber<sup>22</sup> with anomalous dispersions corrections taken from ref 23.

The structure of the compound was solved by direct methods (MULTAN 80). All further stages of the structure determination were carried out by using the SHELX76 program package.<sup>24</sup> Refinement was by full-matrix least-squares calculations, initially with isotropic and then with anisotropic thermal parameters for all non-hydrogen atoms of the complex cation but the phenyl carbon atoms. The function minimized was  $\sum_w (|F_o| - |F_c|)^2$ . No unusual trends were observed in an analysis of the function vs. either  $(\sin \theta)/\lambda$  or  $|F_c|$ . The phenyl rings were treated as rigid groups of  $D_{6h}$  symmetry with C–C distances fixed at 1.395 Å and calculated hydrogen atom positions (C–H = 1.0 Å). Contributions from the remaining hydrogen atoms in positions fixed by geometry have also been taken into account during final cycles of the refinement. At this stage a difference map revealed some higher peaks which were ascribed to a disordered ethanol molecule. The ethanol molecule was found to reside on a crystallographic inversion center  $1/2, 0, 0$ . The inversion center is located midway between the carbon atoms of the ethanol molecule. The carbon atom (C8) was refined isotropically with an occupancy factor of 1.0 and the oxygen atom (O1) of the OH group isotropically with an occupancy 0.5. The bond lengths and angles within the disordered ethanol molecule were C8–C8' = 1.48 (5) Å, C8–O1 = 1.39 (4) Å, and O1–C8–C8' = 144 (3)°. No attempt was made to include hydrogen atoms on the ethanol molecule. The interpretation of the ethanol molecule as disordered around a center of inversion is the only acceptable one, as the assumption of the noncentrosymmetric space group  $P1$  was rejected after a cycle of refinement showed that many of the correlation coefficients between non-solvent atom parameters became unusually high. The largest residual peak on the final difference map was 0.8 e/Å<sup>3</sup> high and was located near the sulfur atom S1.

Final coordinates of all non-hydrogen atoms are reported in Table II.

**Acknowledgment.** Thanks are due to Mr. Franco Ceconi for drawings.

**Registry No.** 1, 53687-39-1; 2, 87306-30-7; 3, 87306-32-9; 4, 85233-91-6; 5, 95911-58-3; 6, 95911-60-7; 6-0.5C<sub>2</sub>H<sub>5</sub>OH, 95977-40-5; 7, 95935-31-2;  $np_3$ , 15114-55-3; CS<sub>2</sub>, 75-15-0;  $[RhCl(C_2H_4)_2]_2$ , 12081-16-2.

**Supplementary Material Available:** Listings of observed and calculated structure factor amplitudes and thermal parameters (20 pages). Ordering information is given on any current masthead page.

(22) "International Tables for X-Ray Crystallography"; Kynoch Press: Birmingham, England, 1974; Vol. IV, p 99.

(23) Reference 22, p 149.

(24) Sheldrick, G. M. SHELX76, Program for Crystal Structure Determinations, University of Cambridge, Cambridge, 1976.